DOI: 10.1002/ejoc.200600543

Computational Study of Reactivity and Transition Structures in Nucleophilic Substitutions on Benzyl Bromides

Ferenc Ruff,*[a] Ödön Farkas,[a] and Árpád Kucsman[a]

Keywords: Nucleophilic substitutions / Benzyl bromides / Substituent effect / Solvent effect / Density functional calculations / Activation parameters

DFT computations on the mechanisms of nucleophilic substitutions on benzyl bromides were performed and the calculated activation parameters were compared with experimentally acquired data. In vacuo, the presence of electron-withdrawing (e-w) groups on the benzyl bromides accelerated the reactions and the calculated $\Delta G^{\ddagger}/\Delta H^{\ddagger}/\Delta S^{\ddagger}$ vs. σ plots were linear, while in solvents there were breaks in the calculated and measured $\Delta G^{\ddagger}/\Delta H^{\ddagger}$ vs. σ^{+} plots of the reactions between the benzyl bromides and Br^{-}, both with electron-donating (e-d) and with e-w substituents accelerating the reactions. The calculated $\Delta S^{\ddagger}$ values appeared to be independent of the substituents. In solvents, the calculated $\Delta G^{\ddagger}/\Delta H^{\ddagger}/\Delta S^{\ddagger}$ vs. σ^{+} plots for the reactions between benzyl bromides and pyridine were linear, whereas breaks were observed in the plots of the measured data. These reactions were promoted by e-d substituents, but the measured reactivities of substrates bearing e-w groups were higher than expected. No breaks in the $\Delta G^{\ddagger}/\Delta H^{\ddagger}/\Delta S^{\ddagger}$ vs. σ plots were observed when the substituents on the pyridine nucleophile were changed. The best agreement between the calculated and measured values was obtained for the least solvent-dependent $\Delta G^{\ddagger}$ parameter. The experimentally measured $\Delta S^{\ddagger}$ and $\Delta H^{\ddagger}$ data were influenced by the rearrangement of the solvent molecules. The calculated structural parameters of the transition states (TSs) varied linearly with the substituent constants, with loose and tight distorted trigonal-bipyramidal TSs being formed by benzyl bromides bearing e-d and e-w groups, respectively. The reactions proceeded by S_N2 mechanisms; only the transition structures were changed with the substituents and the media.

Introduction

The mechanisms of nucleophilic substitutions on benzyl halide derivatives have already been widely investigated.[1–5] These bimolecular reactions take place through the attack of the nucleophile on the methylene carbon atom and have curved Hammett plots.[4–8] In the case of charged nucleophiles the reactions are accelerated by the presence both of electron-donating (e-d) and of electron-withdrawing (e-w) substituents on the benzene ring. If the reactants are uncharged nucleophiles, the presence of e-d groups ($\sigma < 0$) in the substrate accelerates the reactions, while that of e-w substituents ($\sigma > 0$) retards them, but the reaction rates of the compounds containing e-w groups are somewhat higher than those expected from a linear Hammett plot (see details in the Discussion).

Different types of mechanisms have been proposed for these reactions. The observed changes in reactivity have been interpreted[9] in terms of opposing e-d resonance and e-w polar effects, without any change in the mechanism or in the structures of the transition states (TSs). On the other hand, studies of kinetic isotope effects have resulted in the proposal of loose and tight TSs[4,10–13] for substrates bearing e-d and e-w substituents, respectively, with a change from an S_N1-like pathway to an S_N2 type, although the observed activation parameters do not seem to be in accordance with this latter mechanism. Greater $\Delta H^{\ddagger}$ and $\Delta S^{\ddagger}$ values would be expected for the S_N1- than for S_N2-type routes, whereas the opposite results were measured.[14] The participation of an ion-pair intermediate and the attack of the nucleophile on that was therefore thought to be a better interpretation of the mechanism.[14] This pathway has also been taken into consideration in other cases.[3,15–17]

In this paper we report on DFT computations relating to nucleophilic substitutions of benzyl bromides with the charged Br^{-} and the uncharged pyridine as nucleophiles. Optimized structures of the reactants and TSs and also the activation parameters were calculated for the reactions of compounds containing e-d and e-w substituents in the substrate or in the nucleophile, in different solvents and in vacuo. Our aim was to acquire data on the structures of the TSs, and hence on the mechanisms of the reactions, and to identify the causes of the unusual substituent effects in these bimolecular nucleophilic substitutions. As a check on the results, the calculated activation parameters were compared with previously published experimentally measured data.

[a] Department of Organic Chemistry, Institute of Chemistry, L. Eötvös University,
P. O. Box 32, 1518 Budapest 112, Hungary
Fax: +36-1-3722-620
E-mail: ruff@chem.elte.hu
Supporting information for this article is available on the WWW under http://www.eurjoc.org or from the author.

The effects of the media on the calculated and measured activation parameters were also taken into consideration.

Activation parameters are used in this paper to characterize changes in reactivity with the substituents and solvents. The $\Delta G^{\ddagger}$, $\Delta H^{\ddagger}$, and $\Delta S^{\ddagger}$ data were found[18–20] to exhibit linear correlations with the Hammett σ substituent constants [Equation (1), $P = G$, H, or S] in several reactions.

$$\Delta P^{\ddagger} = \delta\Delta P^{\ddagger}\sigma + \Delta P^{\ddagger}_{o} \quad (1)$$

$\Delta G^{\ddagger}$, $\Delta H^{\ddagger}$, $\Delta S^{\ddagger}$ and $\Delta G^{\ddagger}_{o}$, $\Delta H^{\ddagger}_{o}$, $\Delta S^{\ddagger}_{o}$ are the activation parameters of the substituted and unsubstituted compounds, respectively. The $\delta\Delta G^{\ddagger}$, $\delta\Delta H^{\ddagger}$, and $\delta\Delta S^{\ddagger}$ reaction constants are the changes in the activation parameters per unit change in the substituent constants: $\delta\Delta G^{\ddagger}$ and $\delta\Delta H^{\ddagger}$ are given in kJ mol^{-1} σ^{-1}, and $\delta\Delta S^{\ddagger}$ in J mol^{-1} K^{-1} σ^{-1}. Equation (1) can also be used for equilibria with the $\Delta G°$, $\Delta H°$, and $\Delta S°$ data. Through use of Hepler's theory,[21] the reaction constants can be divided into internal and external components[18–20] [Equation (2); $P = G$, H, or S], which correspond to the chemical reaction and the rearrangement of the solvent molecules, respectively [Equation (2)].

$$\delta\Delta P^{\ddagger} = \delta\Delta P^{\ddagger}_{int} + \delta\Delta P^{\ddagger}_{ext} \quad (2)$$

The external component of the free energy of activation and the internal component of the entropy of activation were presumed[18–20,22,23] to vary only very slightly with the remote substituents on the aromatic ring [Equations (3) and (4)]. Accordingly, Equations (5), (6), and (7) were obtained for the reaction constants. These mean that the dependencies of the free energy and the entropy of activation on the substituents are governed mainly by the changes in the internal enthalpy of activation of the chemical reaction [Equation (5)] and by the rearrangement of the solvent [Equation (7)], respectively.[18,20,22,23]

$$\delta\Delta G^{\ddagger}_{ext} = \delta\Delta H^{\ddagger}_{ext} - T\delta\Delta S^{\ddagger}_{ext} \approx 0 \quad (3)$$

$$\delta\Delta S^{\ddagger}_{int} \approx 0 \quad (4)$$

$$\delta\Delta G^{\ddagger} \approx \delta\Delta H^{\ddagger}_{int} \quad (5)$$

$$\delta\Delta H^{\ddagger} \approx \delta\Delta H^{\ddagger}_{int} + T\delta\Delta S^{\ddagger}_{ext} \quad (6)$$

$$\delta\Delta S^{\ddagger} \approx \delta\Delta S^{\ddagger}_{ext} \quad (7)$$

Although the validity of Hepler's theory has been questioned in some cases,[22,24] our earlier DFT calculations[20] indicated that it can be regarded as an acceptable approximation in the studied reactions. The computed $\delta\Delta G^{\ddagger}$ parameters were found to approximate well to the least solvent-dependent experimentally measured $\delta\Delta G^{\ddagger}$ data measured in different solvents,[20] supporting the validity of Equations (3) and (5). The solvent effect on reactivity (i.e., on $\Delta G^{\ddagger}$) can be calculated with the applied continuum model. On the other hand, the rearrangement of the solvent molecules cannot be calculated, so the computed and the solvent-dependent experimentally determined $\delta\Delta H^{\ddagger}$ and $\delta\Delta S^{\ddagger}$ reaction constants differ from each other and have to be evaluated separately. The calculated $\Delta S^{\ddagger} \approx$ const. or exhibits only a very small decrease with increasing tightness of the TS if only the remote substituents on the benzene ring are changed in the reaction series,[20] which confirms the validity of Equation (4). For the computed reaction constants $\delta\Delta S^{\ddagger} \approx 0$, and therefore $\delta\Delta G^{\ddagger} \approx \delta\Delta H^{\ddagger}$ was obtained. The experimentally determined $\delta\Delta S^{\ddagger}$ reaction constants are not zero, and depend on the solvent, while the experimentally determined $\delta\Delta H^{\ddagger}$ reaction constant changes with the solvents[20] because it involves contributions both from the chemical reactions and from the solvent rearrangement [Equation (6)]. The experimentally measured $\delta\Delta S^{\ddagger}$ and $\delta\Delta H^{\ddagger}$ reaction constants can be interpreted by taking account of the changes in the charges and solvation of the TSs and reactants. According to Equation (3) the effects of the solvent rearrangement on $\delta\Delta S^{\ddagger}$ and $\delta\Delta H^{\ddagger}$ cancel each other out and do not change the $\delta\Delta G^{\ddagger}$ reaction constant.

Results and Discussions

Exchange Reactions of Benzyl Bromides and 1-Aryl-1-bromoethanes with Bromide Ion

Optimized structures for the reactants (**1**, **2**), ion-dipole complexes (**4**, **5**), and TSs (**6**, **7**), together with the thermodynamic parameters of complex formation and the activation parameters for the exchange reactions of benzyl bromides (**1**) and 1-aryl-1-bromoethanes (**2**) with Br^- (**3**), were calculated at the DFT(B3LYP)/6-31G(d) level in vacuo and in acetone solution (see details in the Computational Methods Section). The computed activation parameters were compared with the results of kinetic measurements on the reactions of benzyl bromides[25] (**1**) and 1-aryl-1-bromoethanes[14] (**2**) with LiBr in ethane-1,2-diyl diacetate or acetone as solvent, respectively (Scheme 1). The X substituents of the compounds involved in the calculations and in the kinetic measurements for the various reactions are shown in Figures 1–7, while structural parameters of the TSs are plotted in Figures 1–4. Additional structural data are listed in Tables S1 and S2 in the Supporting Information.

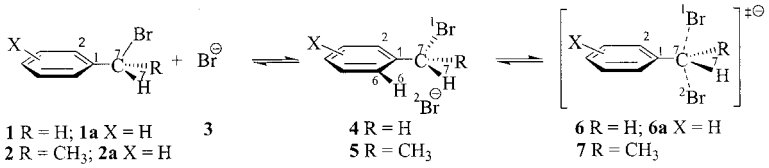

Scheme 1. Ion-dipole complex formations and exchange reactions of benzyl bromides (**1**) and 1-aryl-1-bromoethanes (**2**) with bromide ion (**3**) (X substituents are given in Figures 1–7).

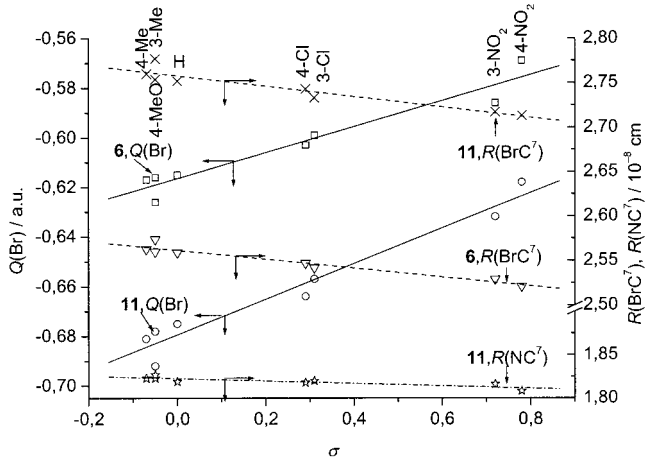

Figure 1. Plots of the calculated charges (Q) and bond lengths (R) of TSs **6** and **11** against the σ constants for the reactions $XC_6H_4CH_2Br + Br^- \leftrightarrows$ TS **6** and for $XC_6H_4CH_2Br + C_5H_5N \leftrightarrows$ TS **11**, in vacuo, at 298 K. The σ constants were determined in the gas phase.[26] X = 4-CH_3, 4-CH_3O, 3-CH_3, H, 4-Cl, 3-Cl, 3-NO_2, 4-NO_2. [Correlations for the data for TS **6**: $Q(Br) = 0.0522\sigma - 0.617$ ($r = 0.967$); $R(BrC^7) = -0.0500\sigma + 2.561$ ($r = 0.966$); for the data for TS **11**: $Q(Br) = 0.0714\sigma - 0.679$ ($r = 0.977$), $R(BrC^7) = -0.0586\sigma + 2.757$ ($r = 0.938$), $R(NC^7) = -0.0142\sigma + 1.823$ ($r = 0.868$)].

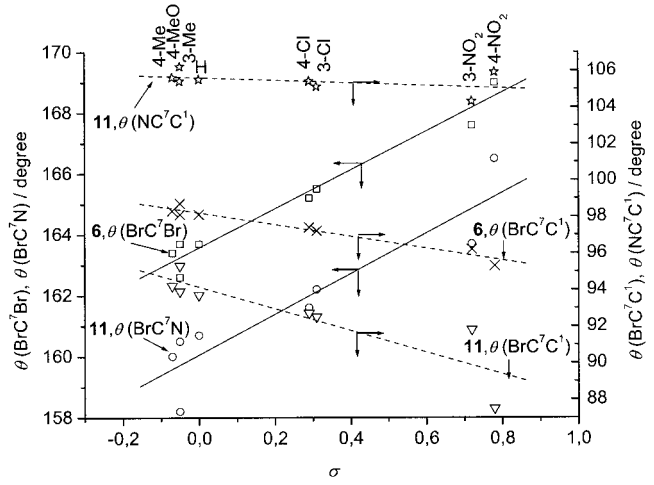

Figure 2. Plots of the calculated bond angles (θ) of the TSs **6** and **11** against the σ constants for the reactions $XC_6H_4CH_2Br + Br^- \leftrightarrows$ TS **6** and for $XC_6H_4CH_2Br + C_5H_5N \leftrightarrows$ TS **11**, in vacuo, at 298 K. The σ constants were determined in the gas phase.[26] X = 4-CH_3, 4-CH_3O, 3-CH_3, H, 4-Cl, 3-Cl, 3-NO_2, 4-NO_2. [Correlations for data for TS **6**: $\theta(BrC^7Br) = 6.39\sigma + 164$ ($r = 0.979$), $\theta(BrC^7C^1) = -3.23\sigma + 98.2$ ($r = 0.974$); for the data for TS **11**: $\theta(BrC^7N) = 6.65\sigma + 160$ ($r = 0.921$), $\theta(BrC^7C^1) = -5.95\sigma + 94.1$ ($r = 0.874$), $\theta(NC^7C^1) = -0.702\sigma + 105.6$ ($r = 0.433$)].

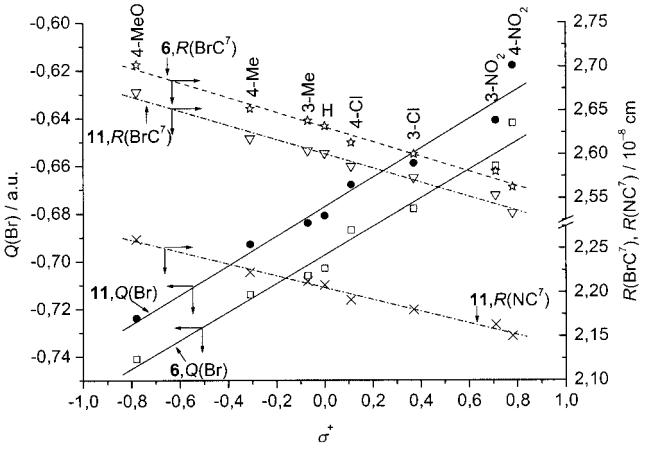

Figure 3. Plots of the calculated charges (Q) and bond lengths (R) of the TSs **6** and **11** against the σ^+ constants[27] for the reactions $XC_6H_4CH_2Br + Br^- \leftrightarrows$ TS **6** and for $XC_6H_4CH_2Br + C_5H_5N \leftrightarrows$ TS **11**, in acetone, at 298 K. X = 4-CH_3O, 4-CH_3, 3-CH_3, H, 4-Cl, 3-Cl, 3-NO_2, 4-NO_2. [Correlations for the data for TSs **6**: $Q(Br) = 0.0598\sigma^+ - 0.697$ ($r = 0.986$), $R(BrC^7) = -0.084\sigma^+ + 2.631$ ($r = 0.992$); for the data for TSs **11**: $Q(Br) = 0.0617\sigma^+ - 0.677$ ($r = 0.984$), $R(BrC^7) = -0.0813\sigma^+ + 2.600$ ($r = 0.988$), $R(NC^7) = -0.0673\sigma^+ + 2.205$ ($r = 0.994$)].

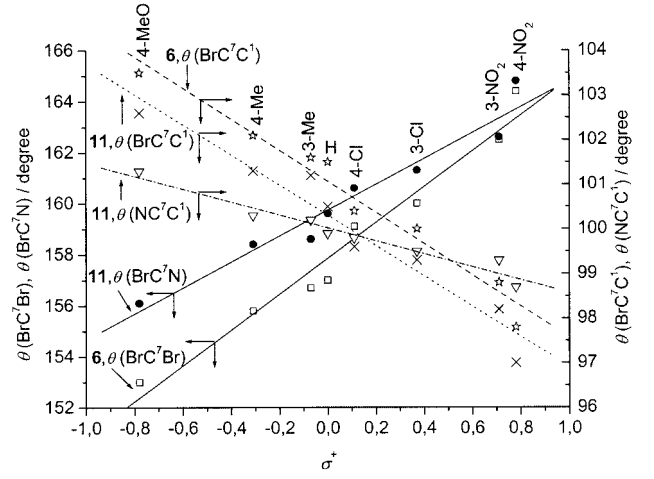

Figure 4. Plots of the calculated bond angles (θ) of the TSs **6** and **11** against the σ^+ constants[27] for the reactions $XC_6H_4CH_2Br + Br^- \leftrightarrows$ TS **6** and for $XC_6H_4CH_2Br + C_5H_5N \leftrightarrows$ TS **11**, in acetone, at 298 K. X = 4-CH_3O, 4-CH_3, 3-CH_3, H, 4-Cl, 3-Cl, 3-NO_2, 4-NO_2. [Correlations for the data for TS **6**: $\theta(BrC^7Br) = 7.02\sigma^+ + 158$ ($r = 0.983$), $\theta(BrC^7C^1) = -3.49\sigma^+ + 101$ ($r = 0.982$); for the data for TS **11**: $\theta(BrC^7N) = 5.07\sigma^+ + 160$ ($r = 0.973$), $\theta(BrC^7C^1) = -3.39\sigma^+ + 100$ ($r = 0.971$), $\theta(NC^7C^1) = -1.45\sigma^+ + 100$ ($r = 0.974$)].

The calculations indicated that in the ion-dipole complexes **4** and **5** the Br^- is located in the vicinity both of the H^6 atom on the aromatic ring and of the H^7 atom in the CHRBr group [$R(Br^2H^7) \approx 2.8$ Å, $R(Br^2H^6) \approx 3.0$ Å in acetone] and is near to the plane of the aromatic ring [$\varphi(Br^2C^6C^1C^2) \approx 175°$].

The TSs **6** formed in the reactions between benzyl bromides (**1**) and Br^- (**3**) assume distorted trigonal-bipyramidal (TBP) geometries. The $Br^1\cdots C^7\cdots Br^2$ atoms deviate from linear arrangements [$\theta(Br^1C^7Br^2) \approx 160°$], and their planes are perpendicular to the aromatic rings [$\varphi(Br^1C^7C^1C^2) \approx 90°$, $\varphi(H^7C^7C^1C^2) \approx 180°$]. In the TSs **7**, formed in the analogous reactions of 1-aryl-1-bromoethanes (**2**), the $CHCH_3$ groups lie in common equatorial planes with the aromatic rings [$\varphi(H^7C^7C^1C^2) \approx 180°$, $\varphi(CH_3C^7C^1C^2) \approx 0°$]. The Br atoms move toward the H^7 atoms, and the Br–C^7 bonds are not perpendicular to the aromatic rings [$\varphi(Br^1C^7C^1C^2) \approx 101°$, $\varphi(Br^2C^7C^1C^2) \approx -102°$].

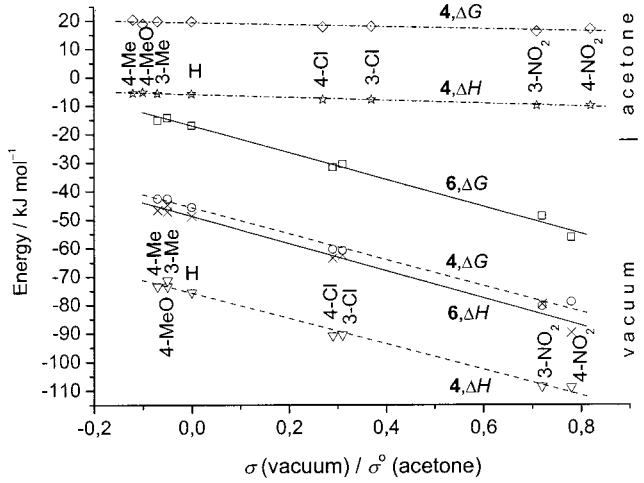

Figure 5. Calculated $\Delta G°/\Delta H°$ vs. σ plots for the equilibria $XC_6H_4CH_2Br + Br^- \leftrightarrows$ **4**, and also the $\Delta G^‡/\Delta H^‡$ vs. σ plots for the exchange reactions $XC_6H_4CH_2Br + Br^- \leftrightarrows$ TS **6**, in vacuo, together with the calculated $\Delta G°/\Delta H°$ vs. $\sigma°$ plots for the equilibria $XC_6H_4CH_2Br + Br^- \leftrightarrows$ **4**, in acetone, at 298 K. X = 4-CH_3, 4-CH_3O, 3-CH_3, H, 4-Cl, 3-Cl, 3-NO_2, 4-NO_2. The σ constants, determined in the gas-phase,[26] and the $\sigma°$ constants[27] were used in vacuo and in acetone, respectively. Reaction constants are given in Table 1, Nos. 1–3.

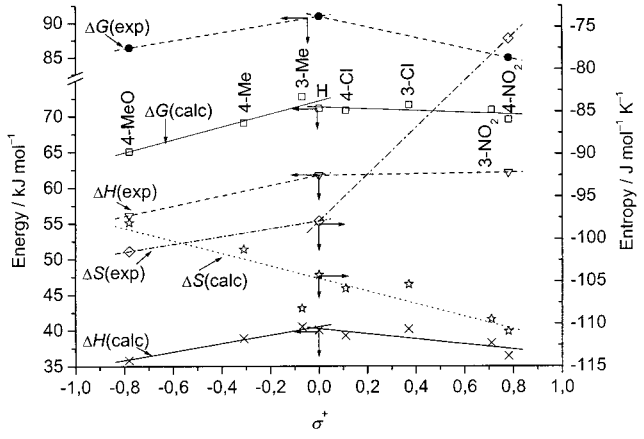

Figure 6. Calculated and experimentally derived $\Delta G^‡/\Delta H^‡/\Delta S^‡$ vs. σ^+ plots for the reactions $XC_6H_4CH_2Br + Br^- \leftrightarrows$ TS **6**, in acetone (calcd) and ethane-1,2-diyl diacetate (exp) solutions, at 298 K. X = 4-CH_3O, 4-CH_3, 3-CH_3, H, 4-Cl, 3-Cl, 3-NO_2, 4-NO_2 for the calculated data, and X = 4-CH_3O, H, 4-NO_2 for the experimental data. Reaction constants are given in Table 1, Nos. 4a,b.

The structural parameters of the TSs **6** display linear correlations with the substituent constants. In vacuo (Figures 1 and 2), the σ constants determined for gas-phase reactions[26] were applied, while in acetone solution (Figures 3 and 4) the σ^+ constants[27] were used. The same substituent constants were utilized in the correlations of the activation parameters. [To permit comparison of the structural parameters of the TSs formed with charged and with uncharged nucleophiles, the data for the TSs **11** involved in the reactions between benzyl bromides (**1**) and pyridine (**10a**) are also plotted in Figures 1–4.] With increasing e-w effects of the X substituents, the Q(Br) negative charges of the Br

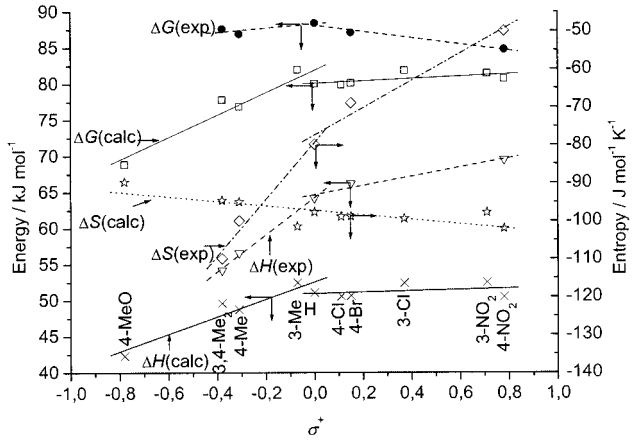

Figure 7. Calculated and experimentally derived $\Delta G^‡/\Delta H^‡/\Delta S^‡$ vs. σ^+ plots for the reactions $XC_6H_4CHBrCH_3 + Br^- \leftrightarrows$ TS **7** in acetone solution, at 298 K. X = 4-CH_3O, 3,4-$(CH_3)_2$, 4-CH_3, 3-CH_3, H, 4-Cl, 4-Br, 3-Cl, 3-NO_2, 4-NO_2 for the calculated data, and X = 3,4-$(CH_3)_2$, 4-CH_3, H, 4-Br, 4-NO_2 for the experimental data. Reaction constants are given in Table 1, Nos. 6a,b.

atoms, the R(BrC^7) distances, and the θ(BrC^7C^1) angles decrease, the θ($Br^1C^7Br^2$) angles increase, and the Br atoms move towards the C^7 atoms and the aromatic rings in both media. (Charges and bond lengths are plotted in Figures 1 and 3, bond angles in Figures 2 and 4.) The TSs become tighter and less polar for compounds with strongly e-w groups. In acetone, the shifts caused by the substituents are larger, and more polar and looser TSs are formed than in vacuo (Figures 1–4). The TSs vary both with the X substituents and with the medium, but distorted TBP structures are formed even if a strongly e-d 4-CH_3O group is linked to the aromatic ring.

In vacuo, the calculated free energies and enthalpies of the ion-dipole complexes **4** and TSs **6** are lower than those obtained for the reactants **1** and **3**, so the $\Delta G°$, $\Delta H°$, $\Delta G^‡$, and $\Delta H^‡$ parameters are therefore negative (Figure 5, Table 1, Nos. 1 and 2). The delocalization of the charges promotes the formation of these species in vacuo. The formation of TSs **6** from the complexes **4** needs activation because the energy levels of TSs **6** are ca. 27 kJ mol^{-1} higher. The calculated $\Delta G°$, $\Delta H°$, $\Delta G^‡$, and $\Delta H^‡$ values correlated well with the σ substituent constants[26] (Figure 5) determined for gas-phase reactions. In vacuo, the formation of the ion-dipole complexes and the exchange reactions are promoted by e-w effects of the substituents ($\delta\Delta G < 0$, $\delta\Delta H < 0$) and were found to be isoentropic ($\delta\Delta S \approx 0$, and therefore $\delta\Delta G \approx \delta\Delta H$; Table 1, Nos. 1 and 2).

The calculations revealed that the equilibrium formation of complexes **4** and **5** in acetone proceeds with a small decrease in enthalpy ($\Delta H° < 0$), but with an increase in free energy ($\Delta G° > 0$), as a consequence of the large decrease in entropy ($\Delta S° < 0$; Table 1, Nos. 3 and 5). The $\Delta G°$ and $\Delta H°$ values in acetone are much larger than those in vacuo (Figure 5, Table 1, No. 1). Earlier studies[28–30] likewise demonstrated that the complex formation during S_N2 reactions is exothermic in vacuo but less exothermic in dipolar

Table 1. Substituent and solvent effects on activation and thermodynamic parameters in the nucleophilic substitution reactions and in the ion-dipole complex formations between benzyl bromides and nucleophiles.[a]

No.	Reaction (Medium)	σ[b]	N[c]	$\delta\Delta G$[d,e] (r)	$\delta\Delta H$[d,e] (r)	$\delta\Delta S$[d,f] (r)	ΔG_o[g,h]	ΔH_o[g,h]	ΔS_o[g,i]
1 (calcd)	**1** + **3** ⇆ **4** (vacuum)	σ	8	–35.7 (0.955)	–34.1 (0.929)	ca. 0	–45.9	–75.5	–100
2 (calcd)	**1** + **3** ⇆ **6** (vacuum)	σ	8	–47.3 (0.996)	–48.0 (0.992)	ca. 0	–17.1	–48.8	–106
3 (calcd)	**1** + **3** ⇆ **4** (acetone)	$\sigma°$	8	–3.67 (0.922)	–5.29 (0.993)	–5.43[j]	19.6	–5.85	–85.5
4a (exp)[25]	**1** + **3** ⇆ **6** ($[CH_2OAc]_2$)[k]	$\sigma^+ \geq 0$	2	–7.73	0.50	27.6	90.9	61.7	–97.9
		$\sigma^+ \leq 0$	2	5.81	7.10	4.53			
4b (calcd)	**1** + **3** ⇆ **6** (acetone)	$\sigma^+ \geq 0$	4	–1.26 (0.570)	–3.57 (0.808)	–7.43 (0.905)	71.1[l]	40.0[l]	–104[l]
		$\sigma^+ \leq 0$	5	9.00 (0.958)	5.84 (0.983)	–7.43 (0.905)			
5 (calcd)	**2** + **3** ⇆ **5** (acetone)	$\sigma°$	10	–4.78 (0.895)	–4.85 (0.984)	ca. 0	20.7	–4.17	–83.3
6a (exp)[14]	**2** + **3** ⇆ **7** (acetone)	$\sigma^+ \geq 0$	3	–4.33 (0.983)	6.35 (0.980)	35.9 (0.983)	88.4	64.2	–79.9
		$\sigma^+ \leq 0$	3	2.93 (0.791)	25.7 (0.998)	74.9 (0.988)			
6b (calcd)	**2** + **3** ⇆ **7** (acetone)	$\sigma^+ \geq 0$	6	1.63 (0.642)	0.92 (0.326)	–5.92 (0.787)	80.3[m]	51.1[m]	–97.7[m]
		$\sigma^+ \leq 0$	5	15.5 (0.954)	12.1 (0.949)	–5.82 (0.787)			
7 (calcd)	**1** + **10a** ⇆ **11** (vacuum)	σ	8	–4.75 (0.879)	–5.74 (0.954)	–3.31 (0.381)	164.6	116.4	–162
8a (exp)[34]	**1** + **10a** ⇆ **11** (acetone)	$\sigma^+ \geq 0$	2	0.29	–0.62	–3.06	94.5	50.3	–148
		$\sigma^+ \leq 0$	2	3.70	6.94	10.9			
8b (calcd)	**1** + **10a** ⇆ **11** (acetone)	σ^+	8	7.23 (0.959)	5.40 (0.979)	–6.26 (0.820)	95.5	52.2	–145
9a (exp)[35]	**1** + **10a** ⇆ **11** (methanol)	$\sigma^+ \geq 0$	2	1.60	18.2	55.8	95.7	53.6	–141
		$\sigma^+ \leq 0$	2	3.53	6.75	10.8			
9b (calcd)	**1** + **10a** ⇆ **11** (methanol)	σ^+	8	6.43 (0.970)	6.03 (0.983)	–1.40 (0.259)	93.5	49.9	–146
10a (exp)[37]	**1a** + **10** ⇆ **12** (acetone)	σ	4	10.9 (0.938)	4.88 (0.898)	–20.2 (0.962)	96.2[n]	50.5[n]	–154[n]
10b (calcd)	**1b** + **10** ⇆ **13** (acetone)	σ	8	13.7 (0.966)	12.4 (0.980)	–2.4 (0.354)	94.7	52.3	–142

[a] Schemes 1 and 2, temperature 298 K. [b] The substituent constants for vacuum and solutions were taken from ref.[26] and ref.[27], respectively. [c] Number of compounds. [d] $\delta\Delta G°$, $\delta\Delta H°$, $\delta\Delta S°$ for the equilibrium Nos. 1, 3, 5; $\delta\Delta G^‡$, $\delta\Delta H^‡$, $\delta\Delta S^‡$ for reaction Nos. 2, 4, 6–10. Correlation coefficients (r) are given in parentheses. [e] In kJ mol^{-1} σ^{-1}. [f] In J mol^{-1} K^{-1} σ^{-1}. [g] $\Delta G_o°$, $\Delta H_o°$, $\Delta S_o°$ for the equilibrium Nos. 1, 3, 5; $\Delta G_o^‡$, $\Delta H_o^‡$, $\Delta S_o^‡$ for reaction Nos. 2, 4, 6–10. [h] Data for compounds with unsubstituted aromatic ring are given in kJ mol^{-1}. [i] Data for compounds with unsubstituted aromatic ring are given in J mol^{-1} K^{-1}. [j] Calculated with Equation (1). [k] Ethane-1,2-diyl diacetate solvent. [l] $\Delta G_o^‡$ = 114 kJ mol^{-1}, $\Delta H_o^‡$ = 104 kJ mol^{-1}, $\Delta S_o^‡$ = –36.2 J mol^{-1} K^{-1} were calculated for the reaction **1a** + **9** ⇆ **6a** + **8**. [m] $\Delta G_o^‡$ = 124 kJ mol^{-1}, $\Delta H_o^‡$ = 115 kJ mol^{-1}, $\Delta S_o^‡$ = –29.7 J mol^{-1} K^{-1} were calculated for the reaction **2a** + **9** ⇆ **7a** + **8**. [n] Data calculated with Equation (1).

aprotic solvents, while these complexes are not produced in protic solvents.[31] Formation of the ion-dipole complexes **4** and **5** is promoted by e-w groups ($\delta\Delta G° < 0$, $\delta\Delta H° < 0$; Table 1, Nos. 3 and 5). The calculated $\Delta G°$ and $\Delta H°$ values give linear correlations with the $\sigma°$ substituent constants[27] (Figure 5) because the benzene ring and the Br$^-$ are not in conjugation.[32] The $\Delta S°$ data were found to be practically independent of the X substituents (Table 1, Nos. 3 and 5).

In acetone, the calculated and measured[14,25] activation parameters obtained for the reactions of substituted benzyl bromides (**1**) and 1-aryl-1-bromoethanes (**2**) with Br$^-$ were correlated with the σ^+ constants[27] (Figures 6 and 7). Strong electron donation through conjugation[32] thus takes place between the π orbital of the benzene ring and the Br···C^7···Br bonds of the TSs **6** and **7**. The calculated $\Delta G^‡$/$\Delta H^‡$ vs. σ^+ and the measured $\Delta G^‡$/$\Delta H^‡$/$\Delta S^‡$ vs. σ^+ plots display breaks at $\sigma^+ \approx 0$. The calculated $\Delta S^‡$ data change only slightly with the substituents, because the effect of the solvent reorganization cannot be computed with the applied methods. The measured $\Delta G^‡$ vs. σ^+ plots are concave downward: both e-d and e-w substituents accelerate the reactions and decrease the value of $\Delta G^‡$. On the other hand, the measured $\Delta H^‡$ and $\Delta S^‡$ parameters increase with increasing σ^+ in both reactions. The measured $\Delta S^‡$ values are influenced mainly by the changes in the charges on the Br atoms and the changes in solvation with the X substituents in the TSs; e-w effects of the X substituents reduce the negative charges on the Br atoms (Figure 3) and decrease the solvation of the TSs **6** and **7**, thereby increasing the experimentally ascertained $\Delta S^‡$ values (Figures 6 and 7). The measured $\Delta H^‡$ parameters are increased by the contribution originating from $\Delta S^‡$ [Equation (6)].

The $\Delta G^{\ddagger}_{o}$ and $\Delta H^{\ddagger}_{o}$ values measured for the reactions of the unsubstituted compounds **1a** and **2a** are higher than calculated (Table 1, Nos. 4a,b and 6a,b); that is, the reactions proceed more slowly than calculated. Calculations were performed with free Br^{-}, while kinetic measurements were made with LiBr, which dissociates only slightly in acetone; Br^{-} (**3**) forms a LiBr ion pair (**9**) with Li^{+} (**8**) rather than ion-dipole complexes **4** and **5** with dipolar substrates **1** and **2**. The former equilibrium [Equation (8)] in acetone has more favorable computed thermodynamic parameters ($\Delta G°$ = –43.2 kJ mol^{-1}, $\Delta H°$ = –63.5 kJ mol^{-1}, $\Delta S°$ = –68.0 J mol^{-1} K^{-1}) than the ion-dipole complex formation (Table 1, Nos. 3 and 5).

$$\underset{\mathbf{8}}{Li^{\oplus}} + \underset{\mathbf{3}}{Br^{\ominus}} \rightleftharpoons \underset{\mathbf{9}}{LiBr} \qquad (8)$$

The activation parameters calculated for the reactions of LiBr (**9**) with benzyl bromide (**1a** + **9** ⇆ **6a** + **8**) and with 1-aryl-1-bromoethane (**2a** + **9** ⇆ **7a** + **8**) are much larger than the measured values (Table 1, Nos. 4b and 6b; see data in footnotes [l] and [m]). It is well known that ion pairs react much more sluggishly than free ions,[33] so we assume that free Br^{-} attacks the benzyl bromide substrates in the exchange reaction. As the concentration of free Br^{-} in acetone is much lower than that of LiBr ion pairs, the experimentally determined $\Delta G^{\ddagger}_{o}$ value is higher than the computed one, and it is not correct because it was calculated with the concentration of LiBr.

Reactions between Benzyl Bromides and Pyridine

The optimized structures of the reactants and TSs, together with the activation parameters for the reactions between substituted benzyl bromides (**1**) and pyridine (**10a**), were computed at the DFT(B3LYP)/6-31G(d) level in vacuo and in acetone and methanol as solvents (Scheme 2), and the calculated activation parameters were compared with those obtained from kinetic measurements in solutions.[34,35] The X substituents of the compounds used in the calculations and in the kinetic measurements of the various reactions are given in Figures 8 and 9, while structural parameters of the TSs **11** are plotted in Figures 1–4 and additional structural data are listed in Table S3 in the Supporting Information.

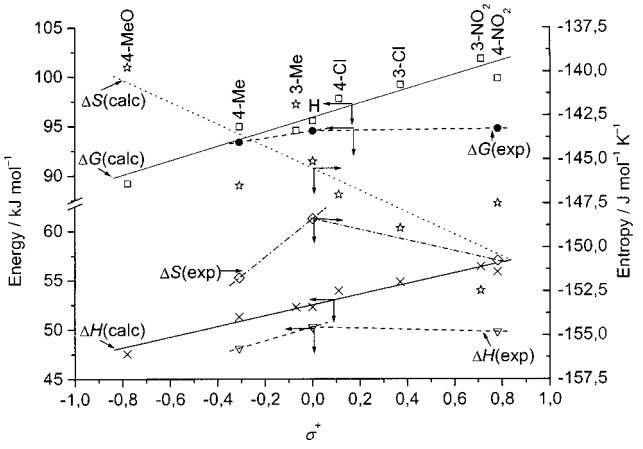

Figure 8. Calculated and experimentally derived $\Delta G^{\ddagger}/\Delta H^{\ddagger}/\Delta S^{\ddagger}$ vs. σ^{+} plots for the reactions $XC_6H_4CH_2Br + C_5H_5N$ ⇆ TS **11**, in acetone solution, at 298 K. X = 4-CH_3O, 4-CH_3, 3-CH_3, H, 4-Cl, 3-Cl, 3-NO_2, 4-NO_2 for the calculated data, and X = 4-CH_3, H, 4-NO_2 for the experimental data. Reaction constants are given in Table 1, Nos. 8a,b.

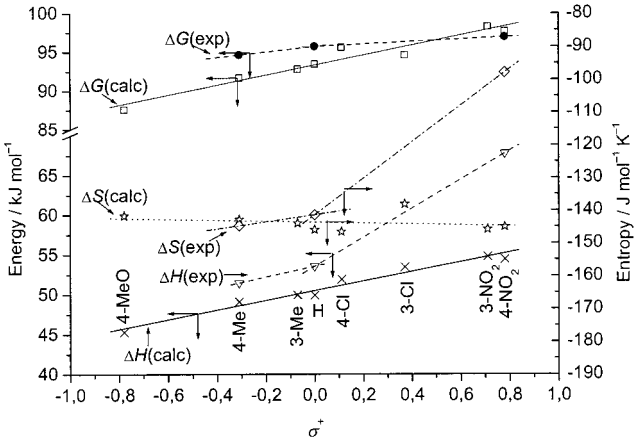

Figure 9. Calculated and experimentally derived $\Delta G^{\ddagger}/\Delta H^{\ddagger}/\Delta S^{\ddagger}$ vs. σ^{+} plots for the reactions $XC_6H_4CH_2Br + C_5H_5N$ ⇆ TS **11** in methanol solution, at 298 K. X = 4-CH_3O, 4-CH_3, 3-CH_3, H, 4-Cl, 3-Cl, 3-NO_2, 4-NO_2 for the calculated data, and X = 4-CH_3, H, 4-NO_2 for the experimental data. Reaction constants are given in Table 1, Nos. 9a,b.

The TSs **11** formed in the reactions between benzyl bromides (**1**) and pyridine (**10a**) exhibit distorted TBP structures; the θ(BrC^7N) bond angles are ca. 160°. With increasing e-d effects of the X substituents ($\sigma < 0$), the negative

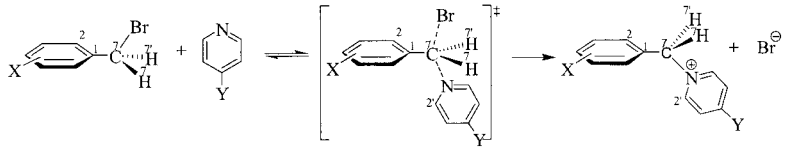

Scheme 2. Reactions between benzyl bromides (**1**) and pyridines (**10**) (X and Y substituents of the compounds are given in Figures 8–10).

Q(Br) charge of the leaving Br, the R(BrC^7) and R(NC^7) distances, and the θ(BrC^{7}C^1) and θ(NC^{7}C^1) bond angles increase, whereas the θ(BrC^{7}N) bond angles decrease (Figures 1–4). In the given series of compounds, the nucleophiles and the leaving groups move further away from the C^7 atom and the benzene ring, so the structures of the TSs become more polar and looser. The structural changes are greater in solvents than in vacuo, and the data furnish linear correlations with the σ^+ constants used for solutions[27] and with the σ constants determined for the gas-phase reactions,[26] respectively (Figures 1–4).

In solution, the planes of the BrC^{7}N atoms in TSs **11** are approximately perpendicular to those of the benzene rings [φ(BrC^{7}C^{1}C^2) ≈ 90°, φ(NC^{7}C^{1}C^2) ≈ –90°]. Strongly e-d interactions occur between the Br···C^7···N bonds and the π orbitals of the benzene rings, which is supported[32] by the correlations of the structural data and the activation parameters with the σ^+ substituent constants.[27] The planes of the attacking pyridine rings do not coincide with the C^1–C^7 bonds. Two energy minima can be found symmetrically, with torsion angles φ(C$^{2'}$NC^{7}C^1) between (5–30)° and –(5–30)° at the C^1–C^7 bond. Librations of the pyridine rings between the two minima may result in slow convergence during the geometry optimization.

In the reactions of benzyl bromides (**1**) with pyridine (**10a**) and with Br$^-$ (**3**), the structures of the TSs **11** and **6** strongly resemble each other in acetone solution (Figures 3 and 4), but differ considerably in vacuo (Figures 1 and 2). This may be explained by comparison of the reaction coordinates (x) of the TSs. Central TSs are formed in the exchange reaction with Br$^-$ in any medium (x = 0.5), and in the reactions with pyridine in solution (x ≈ 0.5). In these cases, the H atoms of the CH_2 group lie approximately in the planes of the benzene rings and do not change their positions appreciably when the X substituent becomes different [φ(H^{7}C^{7}C^{1}C^2) ≈ 180°, φ(H$^{7'}$C^{7}C^{1}C^2) ≈ 0°]. On the other hand, in the late TSs of **11** (x > 0.5) formed in vacuo, the H atoms of the CH_2 groups are bent towards the Br atoms [φ(H^{7}C^{7}C^{1}C^2) < 180°, φ(H$^{7'}$C^{7}C^{1}C^2) > 0°]; the Br···C^7 bonds are longer, and the N···C^7 bonds shorter than in solvent (Figures 1 and 3).

Bond orders for the TS **11a** were calculated according to Pauling [Equation (9)].[36]

$$R - R_o = a \ln(n) \quad (9)$$

By using the Br–C^7 and N–C^7 bond lengths (R_o) in benzyl bromide (**1a**) and *N*-benzylpyridinium ion (**14a**), and the Br···C^7 and N···C^7 bond lengths (R_S) in the symmetric (n = 0.5) TSs **6a** and **15**, respectively, we first calculated the constants a for Equation (9) and then the bond orders n for TS **11a** with the Br···C^7 and N···C^7 bond lengths (R_R). The data in Table 2 indicate that late TSs are formed in vacuo (i.e., the unfavorable formation of ions requires a strong nucleophilic attack). In solvents, earlier TSs are formed because of the stabilization of the charges by the polar media.

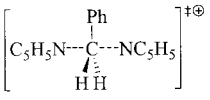

15

Computations relating to vacuum indicated that e-w X groups (σ > 0) decrease the $\Delta G^‡$ values ($\delta\Delta G^‡$ < 0; Table 1, No. 7; Figure S1 in the Supporting Information); that is, they promote the reactions between the benzyl bromides (**1**) and pyridine (**10a**). In contrast, rate-increasing effects of e-d X groups (σ < 0) were observed in solvents. The computed $\Delta G^‡$ values in vacuo are much higher than those measured in solvents (Table 1, Nos. 7, 8a and 9a).

The experimentally determined $\Delta G^‡/\Delta H^‡/\Delta S^‡$ vs. σ^+ plots exhibit breaks for the reactions between benzyl bromides (**1**) and pyridine (**10a**) in acetone and methanol solvents (Figures 8 and 9); e-d effects of the X substituents decrease the $\Delta G^‡$ values, but the measured data for compounds with e-w groups are relatively low (i.e., the rate-reducing effect is not as high as would be expected from a linear correlation). These results are in accordance with previous observations relating to reactions between benzyl halides and uncharged nucleophiles.[7] The experimentally measured $\Delta S^‡$ data may be influenced both by the solvent rearrangement and by the structure of the TS. As mentioned earlier, e-d X substituents increase the negative charge of the leaving Br and therefore also promote the solvation of the TSs, whereas e-w X groups increase the tightness of the TSs (Figures 3 and 4). Both effects may decrease the entropy of activation (Figures 8 and 9). The measured $\Delta H^‡$ data involve contributions from $\Delta S^‡$ [Equation (6)], while the experimentally determined $\Delta H^‡$ vs. σ^+ and $\Delta S^‡$ vs. σ^+ plots are similar.

The computed $\Delta G^‡/\Delta H^‡/\Delta S^‡$ vs. σ^+ plots for these reactions in solvents are linear (Figures 8 and 9), and the $\delta\Delta G^‡$ and $\delta\Delta H^‡$ reaction constants calculated for compounds

Table 2. Bond orders (n)[a] for the TS **11a** generated in the reaction between benzyl bromide and pyridine (Scheme 2).

Medium	Bond	R_S[b,c]	R_o[c,d]	a[e]	R_R[c,f]	n
Vacuum	CN	2.184 (**15**)	1.523 (**14a**)	–0.9536	1.819	0.73
	CBr	2.559 (**6a**)	2.010 (**1a**)	–0.7920	2.752	0.39
Acetone	CN	2.168 (**15**)	1.504 (**14a**)	–0.9581	2.208	0.48
	CBr	2.633 (**6a**)	2.030 (**1a**)	–0.8699	2.600	0.52
Methanol	CN	2.167 (**15**)	1.504 (**14a**)	–0.9572	2.227	0.47
	CBr	2.638 (**6a**)	2.031 (**1a**)	–0.8757	2.592	0.53

[a] Bond orders were calculated according to Pauling [Equation (9)]. [b] Atomic distances [Å] calculated for symmetric TSs (n = 0.5). [c] The numbers of the relating species are given in parentheses. [d] Bond lengths calculated for reactants or products [Å]. [e] Constants calculated for Equation (9). [f] Atomic distances [Å] calculated for the TS **11a**.

substituted with e-d groups ($\sigma < 0$) are more similar to the measured values than those obtained for compounds bearing e-w groups ($\sigma > 0$) (Table 1, Nos. 8a,b and 9a,b). The breaks in the measured $\Delta G^{\ddagger}$ vs. σ^{+} plots cannot be computed with the applied methods, in contrast with the reaction involving the charged Br^{-} nucleophile (see the preceding section). Results are not improved if more extended computational levels are used: values of $\Delta G^{\ddagger}$ = 99.8, 100.2, 99.7, and 94.7 kJ mol^{-1} were calculated for the reaction between 4-nitrobenzyl bromide and pyridine in acetone at the DFT(B3LYP)/6-31G(d), DFT(B3LYP)/6-311G(2d,2p), and MP2/6-311G(d,p) levels and obtained in the kinetic measurements, respectively. One of the reasons for the breaks in the measured $\Delta G^{\ddagger}$ vs. σ^{+} plots may be a non-computed effect of the solvent rearrangement. Inconsistent with this suggestion, though, is the fact that reactions with different types of changes in the measured $\Delta S^{\ddagger}$ vs. σ^{+} plots have the same type of $\Delta G^{\ddagger}$ vs. σ^{+} plots (Figures 8 and 9). Another possible explanation is that the applied solvent continuum model mainly takes the stabilization of charges by the solvent into account. The delocalization of charges by e-w groups could also decrease the energies of the TSs in less polar media, similarly to the situation in vacuo. The decrease in the measured $\Delta G^{\ddagger}$ values for compounds with e-w groups is greater in the less polar acetone than in methanol (see Figures 8 and 9).

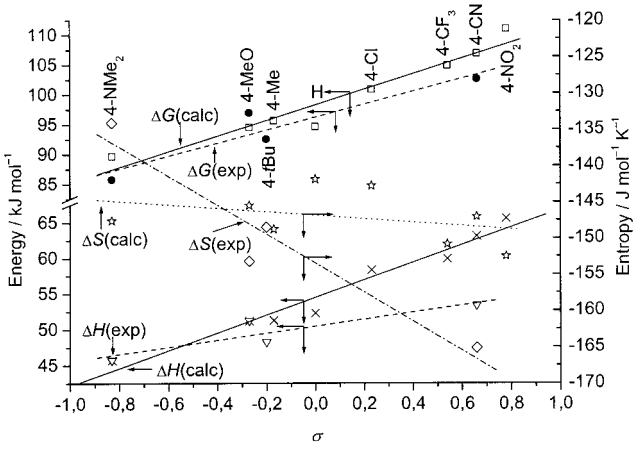

Figure 10. Calculated $\Delta G^{\ddagger}/\Delta H^{\ddagger}/\Delta S^{\ddagger}$ vs. σ plots for the reactions 3-$CH_3C_6H_4CH_2Br$ + YC_5H_4N ⇆ TS **13**, and experimentally derived $\Delta G^{\ddagger}/\Delta H^{\ddagger}/\Delta S^{\ddagger}$ vs. σ plots for the reactions $C_6H_5CH_2Br$ + YC_5H_4N ⇆ TS **12** in acetone solution, at 298 K. The Hammett σ constants[27] determined in solution are used in the correlations. Y = 4-$N(CH_3)_2$, 4-CH_3O, 4-CH_3, H, 4-Cl, 4-CF_3, 4-CN, 4-NO_2 for the calculated data, and Y = 4-$N(CH_3)_2$, 4-CH_3O, 4-$C(CH_3)_3$, 4-CN for the experimental data. Reaction constants are given in Table 1, Nos. 10a,b.

Reactions between 3-Methylbenzyl Bromide and Pyridines

Computations on the nucleophilic substitutions of 3-methylbenzyl bromide (**1b**) with substituted pyridines (**10**) in acetone solution were performed at the DFT(B3LYP)/6-31G(d) level and the obtained activation parameters were compared with those calculated from the results of kinetic measurements[37] for the analogous reactions of benzyl bromide (**1a**) (Scheme 2). Replacement of the 3-H atom with a 3-CH_3 group has only a minor effect on the reactivities and on the structures of the TSs, but on the other hand the 3-CH_3 group hinders the pyridine ring librations between the minima on both sides of the C^1–C^7 bonds, thereby promoting convergence during geometry optimization. The Y substituents of the pyridine nucleophile are given in Figure 10, while the structural parameters of the TSs **13** are plotted in Figures S2 and S3, and listed in Table S4 in the Supporting Information.

The calculated structures for TSs **13** strongly resemble those of TSs **11** (see Figures 3, 4, and Figures S2 and S3 in the Supporting Information), but the effects of the Y substituents of the nucleophile are weaker and the structural changes different from those caused by the X groups on the benzene rings of the substrates. The structural parameters give linear correlations with the Hammett σ constants[27] used for reactions in solution. With increasing e-w effects of the Y groups, the Q(Br) negative charges, the $R(BrC^7)$ distances, and the $\theta(NC^7C^1)$ angles increase, whereas the $R(NC^7)$ distances and the $\theta(BrC^7N)$ and $\theta(BrC^7C^1)$ angles decrease (see Figures S2 and S3 in the Supporting Information). In the given series of nucleophiles, the leaving Br moves away from the C^7 atom and comes slightly closer to the benzene ring, while the attacking pyridine nears the C^7 atom and moves away from the benzene ring. With decreasing nucleophilicity of the pyridines, the H atoms of the CH_2 group move towards the leaving Br [$\varphi(H^7C^7C^1C^2) < 180$, $\varphi(H^{7'}C^7C^1C^2) > 0$]; the reaction coordinates of the TSs become larger ($x > 0.5$), and the TSs are more product-like.

No breaks can be observed either in the calculated or in the measured $\Delta G^{\ddagger}/\Delta H^{\ddagger}/\Delta S^{\ddagger}$ vs. σ plots obtained for the reactions of 3-methylbenzyl bromide (**1b**) and benzyl bromide (**1a**) with pyridines (**10**) (Figure 10). The linear correlations with the σ constants support the notion that the electronic interactions between the lone pairs and the π orbitals of the substituents on the pyridine rings are not very strong.[32] Electron-donating groups ($\sigma < 0$) promote the nucleophilic attack of pyridines, and decrease the values of $\Delta G^{\ddagger}$ and $\Delta H^{\ddagger}$ ($\delta\Delta G^{\ddagger} > 0$, $\delta\Delta H^{\ddagger} > 0$; Table 1, Nos. 10a,b; Figure 10). At the same time, e-w Y groups ($\sigma > 0$) increase the negative charge of the leaving Br (Figure S2 in the Supporting Information) and hence the solvation of the TSs, which results in a decrease in the measured $\Delta S^{\ddagger}$ values ($\delta\Delta S^{\ddagger} < 0$; Table 1, No. 10a; Figure 10). The measured $\Delta H^{\ddagger}$ data are also influenced by the decrease in $\Delta S^{\ddagger}$, according to Equation (6). On the other hand, the calculated $\Delta S^{\ddagger}$ parameter decreases only slightly with increasing e-w effects of the Y substituents, so $\delta\Delta G^{\ddagger} \approx \delta\Delta H^{\ddagger}$ was obtained for the calculated reaction constants.

The calculated and the least solvent-dependent experimentally determined $\delta\Delta G^{\ddagger}$ reaction constants and $\Delta G^{\ddagger}_{o}$, $\Delta H^{\ddagger}_{o}$, and $\Delta S^{\ddagger}_{o}$ activation parameters for the reactions of 3-methylbenzyl bromide (**1b**) and benzyl bromide (**1a**) with

pyridines (**10**) are in good agreement (Table 1, Nos. 10a,b); the weak effect of the X = 3-CH_3 substituent does not change these data markedly.

Conclusions

DFT computations were performed on nucleophilic substitutions of benzyl bromides with the charged Br^- and the uncharged pyridine nucleophiles. Our aim was to study the effects of the substituents and the media on the mechanisms of these reactions. Results were validated by comparison of the computed and measured activation parameters, and the conclusions can be summarized as follows.

1. The calculations revealed that only e-w groups accelerate nucleophilic substitution on benzyl bromides in vacuo, since the delocalization of the charges by e-w groups increases the stabilities of the compounds. On the other hand, e-d substituents on the substrates accelerate the nucleophilic substitutions on benzyl bromides in solutions because the polar solvent molecules can stabilize the polar TSs formed.

2. The computed $\Delta S^{\ddagger}$ data changed only slightly with the remote substituents and the tightness of the TSs. $\delta\Delta S^{\ddagger} \approx 0$ and consequently $\delta\Delta G^{\ddagger} \approx \delta\Delta H^{\ddagger}$ were obtained for the computed reaction constants. The low-frequency vibrations of the reactants and TSs may also influence the $\Delta S^{\ddagger}$ values; these may be the cause of the scattering of the computed data. The measured $\Delta S^{\ddagger}$ values depended on the substituents (i.e., $\delta\Delta S^{\ddagger} \neq 0$) and were influenced by the changes in solvation of the TSs. The formation of solvation shells may increase the ordering of the solvent molecules so that the measured entropies of activation should decrease with increasing charge on the TSs.

3. The experimentally determined $\Delta H^{\ddagger}$ data and $\delta\Delta H^{\ddagger}$ reaction constants contain contributions originating from the chemical reactions and from the rearrangement of the solvents. No firm conclusions concerning the mechanisms of the reactions (e.g., the formation of ion-pair intermediates[14]) can be drawn from the experimentally measured $\Delta H^{\ddagger}$ data because of the solvent dependence of these parameters.

4. The effect of the reorganization of the solvent molecules during the reaction mainly influences the measured $\Delta H^{\ddagger}$ and $\Delta S^{\ddagger}$ values, but does not change the value of $\Delta G^{\ddagger}$ markedly. The changes in the $\Delta H^{\ddagger}$ and $\Delta S^{\ddagger}$ parameters cancel each other: this is the well-known compensation effect.[22] The rearrangement of the solvent molecules cannot be computed, so the measured and calculated values for the $\Delta H^{\ddagger}$ and $\Delta S^{\ddagger}$ parameters are different. The $\Delta G^{\ddagger}$ data are influenced mainly by the polarity of the solvent, and this effect can be computed by use of the polarizable continuum model. The $\Delta G^{\ddagger}$ parameter can be calculated with acceptable accuracy, especially for reactions of nonpolar molecules in aprotic solvents. The application of a solvent model is therefore a necessary condition for the calculation of transition structures and reactivities (i.e., $\Delta G^{\ddagger}$ data) in solutions. Excellent new methods for the calculation of free energies of activation in solvents have already been published,[39] but we have found that satisfactory results for $\Delta G^{\ddagger}$ data can also be obtained by use of the Gaussian program with the solvent continuum model. Because of the large number of computations needing to be carried out, our only option was to use a well-established method with moderate computational demand.

5. The calculated charges, bond lengths, and bond angles in the TSs give linear correlations with exactly the same substituent constants as used in the correlations of the activation parameters, although there are breaks in the plots of the activation parameters. Late and central TSs are formed in vacuo and in solutions, respectively.

6. In accordance with the results of earlier investigations on kinetic isotope effects,[4,10–13] we found that the S_N2 mechanism in the nucleophilic substitutions of benzyl bromides does not alter with the substituents: only the structures of the TSs are modified. Tight TBP-like TSs are formed from substrates bearing e-w substituents, in which both the nucleophile and the leaving group form relatively strong bonds. On the other hand, loose distorted TBP-like TSs are formed from benzyl bromides bearing e-d substituents. In the latter cases, both the entering and the leaving groups are weakly bonded to the reaction center, and "soft" attack by the nucleophile is sufficient to expel the leaving group. Similar changes in the TSs could not be calculated when the substituents were varied in the pyridine nucleophile. We therefore propose that concerted substituent and solvent effects cause the changes in the reactivities of benzyl substrates with the substituents. If the substituted aromatic ring of the substrate is bonded directly to the reaction center, downward curved $\Delta G^{\ddagger}$ vs. σ plots with breaks at $\sigma \approx 0$ can be obtained not only when there is a change in the reaction mechanism,[32,38] but also when the structure and the solvation of the TSs vary with the substituents.

Computational Methods

The geometry of each compound was fully optimized without symmetry constraints by use of the Gaussian 03 software package[40] at the DFT(B3LYP)/6-31G(d) level, at 298 K. All structures were characterized as energy minima or TSs by calculation of the harmonic vibration frequencies, with no or one imaginary frequency for reactants and TSs, respectively, with use of analytical second derivatives. The solvent effect was incorporated by application of the polarizable continuum model[41] in the integral equation formalism[42,43] (IEF-PCM) of the corresponding solvent. Selected data for the optimized structures obtained by DFT calculations are plotted in Figures 1–4, Figures S2 and S3 and listed in Tables S1–S4 in the Supporting Information. The thermochemical data were obtained by the standard procedure in the framework of the harmonic approximation.[44,45] The sums of the electronic and thermal free energies (G) and enthalpies (H) and also the entropies of formation (S) for reactants and TSs are listed in Tables S5 and S6 in the Supporting Information. The entropy (S) values for a compound computed in vacuo and in different solutions are almost equal, and agree well with the data obtained by application of Benson's rule[46] in the gas phase. As an example, S values of 372.8, 370.7, and 370.7 $J\,mol^{-1}\,K^{-1}$ were obtained for $C_6H_5CH_2Br$ by DFT calculations in vacuo and subsequently in acetone and meth-

anol solutions, respectively. In comparison, a value of S = 374 J mol^{-1} K^{-1} was calculated at 25 °C on application of Benson's rule. The $\Delta G^{\ddagger}$, $\Delta H^{\ddagger}$, and $\Delta S^{\ddagger}$ parameters for the reactions, and the $\Delta G°$, $\Delta H°$, and $\Delta S°$ values for equilibria were calculated from the differences in the G, H, and S values of the TSs or products and reactants, respectively. In these calculations, the data obtained by DFT computations at the B3LYP/6-31G(d) level (listed in Tables S5 and S6 in the Supporting Information) were used. The generated $\Delta G^{\ddagger}$ and $\Delta H^{\ddagger}$ values were multiplied by 627.51 and 4.184 in order to convert them into kJ mol^{-1} units. For the purpose of method validation, higher level [DFT(B3LYP)/6-311G(2d,2p) or MP2/6-311G(d,p)] calculations were used for final single-point energy calculations in the case of the reaction between 4-nitrobenzyl bromide and pyridine. The total energy values were combined with the B3LYP/6-31G(d) thermochemical contributions to obtain the G data (see footnotes of Tables S5 and S6 in the Supporting Information). The $\Delta G^{\ddagger}$ values did not change significantly when the calculations were performed at the extended levels. The $\delta\Delta G^{\ddagger}$, $\delta\Delta H^{\ddagger}$, and $\delta\Delta S^{\ddagger}$ reaction constants were calculated from the activation parameters obtained through the DFT computations and from kinetic measurements by use of Equation (1) as described previously.[18–20] The appropriate substituent constants[27] listed in Table S7 in the Supporting Information, which gave the best correlations with the activation parameters, were used. The σ substituent constants determined for gas-phase reactions[26] were applied for data calculated in vacuo. The $\Delta G^{\ddagger}/\Delta H^{\ddagger}/\Delta S^{\ddagger}$ vs. σ plots of the reactions of benzyl substrates often have two linear components, separately for compounds with e-w and e-d substituents, with breaks at $\sigma \approx 0$. The data for the unsubstituted compound are situated at the crossing-point of the two lines, and seem to belong to both. In these cases the $\delta\Delta G^{\ddagger}$, $\delta\Delta H^{\ddagger}$, and $\delta\Delta S^{\ddagger}$ reaction constants were calculated by use of Equation (1), separately for compounds bearing e-w and e-d substituents. Gaussian input (gjf) files to reproduce the published data for reactants and transition states are available on request from the author.

Supporting Information (see footnote on the first page of this article): Lists of selected atomic charges, bond lengths, bond angles and torsion angles, calculated sums of electronic and thermal free energies and enthalpies, entropies of formation, dipole moments.

Acknowledgments

This work was supported by the Hungarian Scientific Research Foundation (OTKA Nos. 043639 and K 60889).

[1] S. R. Hartshorn, *Aliphatic Nucleophilic Substitution*, Cambridge University Press, Cambridge, **1973**, and references contained therein.
[2] G. Kohnstam, *Adv. Phys. Org. Chem.* **1967**, *5*, 121–169.
[3] R. A. Sneen, *Acc. Chem. Res.* **1973**, *6*, 46–53.
[4] R. A. Y. Jones, *Physical and Mechanistic Organic Chemistry*, 2nd ed., Cambridge University Press, Cambridge, **1984**, pp. 155–158, and references contained therein.
[5] M. B. Smith, J. March, *March's Advanced Organic Chemistry, Reactions, Mechanism, and Structure*, 5th ed., J. Wiley & Sons, New York, **2001**, p. 436, and references contained therein.
[6] a) E. Tommila, I. Pitkänen, *Acta Chem. Scand.* **1966**, *20*, 937–945; b) E. Tommila, M. Savolainen, *Acta Chem. Scand.* **1966**, *20*, 946–962; c) K. Kalliorinne, E. Tommila, *Acta Chem. Scand.* **1969**, *23*, 2567–2572.
[7] T. Thorstenson, R. Eliason, A. Songstad, *Acta Chem. Scand.* **1977**, *A31*, 276–280.
[8] F. P. Ballistreri, E. Maccarone, A. Mamo, *J. Org. Chem.* **1976**, *41*, 3364–3366.
[9] P. R. Young, W. P. Jencks, *J. Am. Chem. Soc.* **1979**, *101*, 3288–3294.
[10] a) E. C. F. Ko, A. J. Parker, *J. Am. Chem. Soc.* **1968**, *90*, 6447–6453; b) E. C. F. Ko, K. T. Leffek, *Can. J. Chem.* **1972**, *50*, 1297–1302.
[11] V. P. Vitullo, J. Grabowski, S. Sridharan, *J. Am. Chem. Soc.* **1980**, *102*, 6463–6465.
[12] J. M. Harris, S. G. Shafer, J. R. Moffatt, A. R. Becker, *J. Am. Chem. Soc.* **1979**, *101*, 3295–3300.
[13] a) K. C. Westaway, S. F. Ali, *Can. J. Chem.* **1979**, *57*, 1359–1367; b) O. Matson, A. Dybala-Defratyk, M. Rostkowski, P. Paneth, C. K. Westaway, *J. Org. Chem.* **2005**, *70*, 4022–4027; and references cited therein.
[14] A. R. Stein, M. Tencer, E. A. Moffatt, A. R. Becker, *J. Org. Chem.* **1980**, *45*, 3539–3540.
[15] a) H. Aronovitch, A. Pross, *J. Chem. Soc., Perkin Trans. 2* **1978**, 540–545; b) Y. Karton, A. Pross, *J. Chem. Soc., Perkin Trans. 2* **1980**, 250–254.
[16] P. Cayzergues, C. Georgoulis, G. Mathieu, *J. Chim. Phys.* **1987**, *84*, 63–70.
[17] A. Streitwieser, E. G. Jayasree, S. S.-H. Leung, G. S.-C. Choy, *J. Org. Chem.* **2005**, *70*, 8486–8491.
[18] F. Ruff, *J. Mol. Struct. (THEOCHEM)* **2002**, *617*, 31–45.
[19] F. Ruff, *Internet Electron. J. Mol. Des.* **2004**, *3*, 474–498. http://www.biochempress.com.
[20] F. Ruff, Ö. Farkas, *J. Org. Chem.* **2006**, *71*, 3409–3416.
[21] a) L. G. Hepler, W. F. O'Hara, *J. Phys. Chem. J. Phys. Chem.* **1961**, *65*, 811–814; b) L. G. Hepler, *J. Am. Chem. Soc.* **1963**, *85*, 3089–3092; c) J. W. Larson, L. G. Hepler, *J. Org. Chem.* **1968**, *33*, 3961–3963; d) L. G. Hepler, *Can. J. Chem.* **1971**, *49*, 2803–2807; e) T. Matsui, L. G. Hepler, *Can. J. Chem.* **1977**, *54*, 1296–1299.
[22] O. Exner, *Prog. Phys. Org. Chem.* **1973**, *10*, 411–482, and references therein.
[23] a) E. Grunwald, C. Steel, *J. Am. Chem. Soc.* **1995**, *117*, 5687–5692; b) E. Gallicchio, M. M. Kubo, R. M. Levy, *J. Am. Chem. Soc.* **1998**, *120*, 4526–4527; c) M. Rekharsky, Y. Inoue, *Chem. Rev.* **1998**, *98*, 1875–1917.
[24] a) T. M. Krigowski, J. Guilleme, B. Wojtkowiak, *J. Chem. Soc., Perkin Trans. 2* **1979**, 1143–1144; b) G. Brethon, M. J. Blais, O. Enea, *J. Phys. Chem.* **1977**, *81*, 1991–1995.
[25] S. Sugden, J. B. Willes, *J. Chem. Soc.* **1951**, 1360–1363.
[26] a) T. B. McMahon, P. Kebarle, *J. Am. Chem. Soc.* **1977**, *99*, 2222–2230; b) R. W. Taft, R. D. Topsom, *Prog. Phys. Org. Chem.* **1987**, *16*, 1–84.
[27] C. Hansch, H. Leo, R. W. Taft, *Chem. Rev.* **1991**, *91*, 165–195.
[28] S. Wolfe, D. J. Mitchell, *J. Am. Chem. Soc.* **1980**, *103*, 7692–7694.
[29] J.-L. M. Abboud, R. Notario, J. Bertran, M. Sola, *Prog. Phys. Org. Chem.* **1993**, *19*, 1–181.
[30] C. Li, D. Ross, J. E. Szulejko, T. B. McMahon, *J. Am. Chem. Soc.* **1996**, *118*, 9360–9367.
[31] W. L. Jorgensen, *Acc. Chem. Res.* **1989**, *22*, 184–189.
[32] F. Ruff, I. G. Csizmadia, *Organic Reactions: Equilibria, Kinetics and Mechanism*, Elsevier, Amsterdam, **1994**, chapter 7, pp. 161–180.
[33] a) J. E. Gordon, *The Organic Chemistry of Electrolyte Solutions*, Wiley, New York. **1975**. pp. 299, 471.; b) C. Reichardt, *Solvent and Solvent Effects, in Organic Chemistry*, 2nd ed., Verlag Chemie, Weinheim, **1988**, pp. 5–55.
[34] J. W. Baker, W. S. Nathan, *J. Chem. Soc.* **1935**, 519–527.
[35] P. Haberfield, A. Nudelman, A. Bloom, R. Romm, H. Ginsberg, *J. Org. Chem.* **1971**, *36*, 1792–1795.
[36] L. Pauling, *J. Am. Chem. Soc.* **1947**, *69*, 542–553.
[37] R. M. Claramunt, R. Gallo, J. Elquero, D. Mathieu, R. Phan Tau Luu, *J. Chim. Phys. Phys.-Chim. Biol.* **1981**, *78*, 805–814.
[38] O. Exner, *Correlation Analysis of Chemical Data*, Plenum, New York, **1988**.

[39] a) P. G. Bolhuis, D. Chandler, C. Dellago, P. L. Geissler, *Annu. Rev. Phys. Chem.* **2002**, *53*, 291–318; b) G. Ciccotti, R. Kapral, E. Vanden-Eijnden, *ChemPhysChem* **2005**, *6*, 1809–1814.
[40] M. J. Frisch, G. W. Trucks, H. B. Schlegel, G. E. Scuseria, M. A. Robb, J. R. Cheeseman, J. A. Montgomery Jr, T. Vreven, K. N. Kudin, J. C. Burant, J. M. Millam, S. S. Iyengar, J. Tomasi, V. Barone, B. Mennucci, M. Cossi, G. Scalmani, N. Rega, G. A. Peterson, H. Nakatsuji, M. Hada, M. Ehara, K. Toyota, R. Fukuda, J. Hasegawa, M. Ishida, T. Nakajima, Y. Honda, O. Kitao, H. Nakai, M. Klene, X. Li, J. E. Knox, H. P. Hartchian, J. B. Cross, C. Adamo, C. Jaramillo, R. Gomperts, R. E. Stratmann, O. Yazyev, A. J. Austin, R. Cammi, C. Pomelli, J. W. Ochterski, P. Y. Ayala, K. Morokuma, G. A. Voth, P. Salvador, J. J. Dannenberg, V. G. Zakrzewski, S. Daprich, A. D. Daniels, M. C. Strain, Ö. Farkas, D. K. Malick, A. D. Rabuck, K. Raghavachari, J. B. Foresman, J. V. Ortiz, Q. Cui, A. G. Baboul, S. Clifford, J. Cioslowski, B. B. Stefanov, G. Liu, A. Liashenko, P. Piskorz, I. Komáromi, R. L. Martin, D. J. Fox, T. Keith, L. A. Al-Laham, C. Y. Peng, A. Nanayakkara, M. Challacombe, P. M. W. Gill, B. Johnson, W. Chen, M. W. Wong, C. Gonzalez, J. A. Pople, *Gaussian 03*, revision C.02, Gaussian, Inc., Pittsburg, PA, **2003**.
[41] J. Tomasi, M. Persico, *Chem. Rev.* **1994**, *94*, 2027–2094.
[42] E. Cancès, B. Mennucci, *J. Chem. Phys.* **2001**, *114*, 4744–4745.
[43] D. M. Chipman, *J. Chem. Phys.* **2000**, *112*, 5558–5565.
[44] D. A. McQuarrie, J. D. Simon, *Molecular Thermodynamics*, University Science Books, Sausalito, CA, **1999**.
[45] http://www.gaussian.com/g_whitepap/thermo/thermo.pdf.
[46] a) S. W. Benson, F. R. Cruickshank, D. M. Golden, G. R. Haugen, H. E. O'Neal, A. S. Rodgers, R. Shaw, R. Walsh, *Chem. Rev.* **1969**, *69*, 279–290; b) S. W. Benson, *Thermochemical Kinetics*, Wiley, New York, **1976**, pp. 19–72.

Received: June 23, 2006
Published Online: October 23, 2006

